High-Fat Diet And High Blood Insulin Level Impair Fat Taste Perception And Disrupt Metabolism In Type 2 Diabetic C57BL/6J Mice

Lynda Hamedi[1], Djamil Krouf[1*], Karima Dahili[1], Aziz Hichami[2], Amira Sayed Khan[2], Naim Khan[2]

[1]Laboratory of Clinical and Metabolic Nutrition (LNCM), Faculty of Nature and Life Sciences, University of Oran 1 Ahmed Ben Bella, BP 1524 El M'Naouer, 31100 Oran, Algeria
[2]NUTox Team, UMR INSERM 1231, "CTM", university of burgundy Europe, 6 Bd Gabriel, Dijon – 21000, France
**Corresponding author: Prof. Djamil Krouf*
E-mail address: krouf.djamil@univ-oran1.dz; lncmkrouf@gmail.com.
ORCID: https://orcid.org/0000-0003-2159-9422

KEYWORDS

Mice, Diabetes, High Fat Diet, Insuline, TBC, Calcium signaling, oxidative stress, inflammation

ABSTRACT:

Introduction: Type 2 diabetes (T2D), frequently accompanied by hyperinsulinemia, is associated with impaired taste sensitivity, which may affect dietary preferences and metabolic health.

Objectives: This study investigates how a high-fat diet (HFD) and hyperinsulinemia influence fat taste perception through disruptions in calcium signaling, while also assessing key metabolic parameters such as glucose homeostasis, lipid profiles, oxidative stress, and inflammation in male C57BL/6J mice.

Methods: Mice (n=24) were fed either standard (STD) or high-fat diet (HFD) for 15 days, then subdivided into control, HFD, STZ, and HFD-STZ groups (n=6 each). T2D was induced in STZ and HFD-STZ mice via streptozotocin injections (40 mg/kg/bw/day, i.p). Fatty acid preference was evaluated using a two-bottle choice test, and calcium imaging was performed on isolated taste bud cells (TBC). Plasma lipid profiles, TBARS, SOD, GPx, TNF-α, IL-1β, and IL-6 levels were analyzed.

Results: The STZ group showed increased food and energy intake, while the HFD and HFD-STZ groups exhibited reduced food intake but elevated energy consumption. Glycemia and insulinemia were significantly higher in the HFD, STZ and HFD-STZ groups, with the HFD-STZ and mice displaying insulin resistance. Alterations in lipid profiles and oxidative stress markers were evident, particularly in the HFD and HFD-STZ groups, which also demonstrated elevated pro-inflammatory cytokines and reduced antioxidant activity. Our results revealed a decreased preference for fat in the HFD and HFD-STZ groups, which correlated with suppressed calcium signaling triggered by linoleic acid (LA). Also, the STZ group exhibited a slight preference for the fat solution, with a reduced calcium response in TBC.

Conclusions: These findings highlight the pivotal role of hyperinsulinemia, inflammation and oxidative stress associated to diabetes in impairing fat taste sensitivity and disrupting dietary regulation, emphasizing the importance of managing insulin levels for glycemic control and preserving sensory mechanisms crucial for healthy eating behaviors.

1. Introduction

Diabetes is a complex syndrome characterized by chronic hyperglycemia and is classified into type 1 diabetes (T1D), type 2 diabetes (T2D), specific forms of diabetes, and gestational diabetes mellitus (ADAPPC, 2024). Among these, T2D accounts for approximately 90% of all cases (Sun et al., 2022) and is marked by a progressive, non-autoimmune decline in the insulin-secreting capacity of pancreatic beta cells. This dysfunction is often accompanied by insulin resistance (IR) and metabolic syndrome (MS), both central to T2D pathogenesis. Pancreatic beta cells, the primary source of insulin, play a critical role in maintaining

glucose homeostasis by synthesizing, storing, and releasing insulin in response to metabolic fluctuations (Bartolomé, 2023).

Unbalanced dietary patterns, particularly high-calorie Western diets, significantly contribute to beta-cell dysfunction. These diets promote dyslipidemia and oxidative stress, activating proinflammatory pathways that exacerbate insulin resistance and accelerate the progression of T2D (Galicia-Garcia, 2020).

Experimental studies have shed light on the mechanisms underlying T2D. High-fat diets in mice induce insulin resistance and hyperinsulinemia without necessarily causing hyperglycemia (Varghese et al., 2020). Moreover, combining HFD with low-dose streptozotocin (STZ) effectively induces T2D in animal models, although outcomes vary depending on diet composition, STZ dosage, species, and age (Sing, 2024). The interaction between HFD and STZ exacerbates metabolic dysfunctions, including systemic inflammation and oxidative damage, pivotal factors in T2D development. Fernandez-Millan et al. (2022) emphasized the importance of inter-organ communication in T2D, particularly how beta cells interact with metabolic and non-metabolic tissues, paving the way for novel research avenues.

In addition to its impact on metabolic regulation, diabetes profoundly influences sensory functions, notably taste perception. This sensory process, governed by receptors located within the digestive tract, is essential for maintaining balanced food intake. Disruptions in taste perception can lead to imbalanced eating behaviors, contributing to malnutrition, overnutrition, and metabolic pathologies linked to prolonged high-fat diet consumption (Peinado et al., 2023).Studies consistently demonstrate a negative correlation between dietary fat consumption and fat taste sensitivity, with HFD consumers exhibiting diminished sensitivity to fat taste (Khan et al., 2020).

Humans and rodents show a spontaneous preference for dietary lipids. Several studies suggest the existence of fat taste of as a sixth taste modality for the orosensory detection of dietary long-chain fatty acids (LCFAs) (Khan et al., 2020). CD36 and GPR120receptors located in taste bud cells (TBC), play a crucial role in the fat detection. LCFAs activation of these receptors triggers an increase in intracellular calcium concentration allowing the release of neurotransmitter which, by activating the afferent nerves, transmits fat-taste signal to the nucleus of solitary tract and the gustatory brain areas (Hichami et al., 2022)

Diabetes, particularly T2D with elevated insulin blood level, directly impairs taste sensitivity. Indeed, researchers have explored the potential impact of diabetes on taste sensitivity, revealing that changes in taste perception may influence the dietary choices of diabetic patients (Takai and Shigemura, 2020). Furthermore, Rohde et al. (2020) highlighted the importance of targeting taste receptors and sensory pathways as potential therapeutic strategies to mitigate diabetes-induced changes in food preferences and metabolic outcomes.

Various hypotheses have been proposed to elucidate the association between fat-taste perception and obesity, including hedonic appetite, alterations in gut microbiota, impaired taste sensitivity, and elevated taste thresholds. However some studies have identified significant correlations between fat-taste perception and obesity, others report inconclusive findings, underscoring the complexity of this relationship. In light of these intricacies, this study aimed to investigate how HFD combined with T2D, influences fat perception in TBC through disruptions in calcium signaling. Additionally, we assessed metabolic parameters, including body weight, glucose homeostasis, lipid profiles, oxidative stress markers, and inflammatory responses, using male C57BL/6J mice as the experimental model.

2. Methods

2.1. Animal model and experimental design:

Experiments were performed using The C57BL/6J male mice, purchased from Janvier lab (France). Animals were housed in suitable cages with a controlled environment (12h light/dark photocycle with constant temperature 25°C and humidity 60±5%). The study was conducted in accordance with the Declaration of Helsinki and European ethical guidelines regarding the care and use of animals in experimentation. All experimental protocols received approval from the Regional Ethical Committee of the University of Burgundy (Dijon, France). Twenty-four mice (n=24), with an average weight of 25.44±0.42 g, were randomly divided into two equal groups (n=12): a control group fed with standard diet (STD) and HFD group consumed high fat diet (HFD)(**Table 1**).

Table 1. Composition of the diets.

Ingredients	Standard diet (%)	High-calorie diet (HFD) (%)

Starch	66.80	40.07
Proteins	16.10	14.60
Fats	3.10	35.30
Cholesterol	-	0.03
Cellulose	3.90	2.70
Vitamins[b]	2.70	3.40
Minerals[c]	5.10	3.90
Total energy (Kcal/100g diet)	359.5	536.65
Fat energy[a] (% of total energy)	8.00	60

The diets were prepared in laboratory. The fatty acids composition of fats (%) in standard diet is 18.82 % saturated fatty acids (SFA), 26.38% monounsaturated fatty acids (MUFA) and 54.80% polyunsaturated fatty acids (PUFA). High-fat diet (HFD) contained 45.85% SFA, 40.02% MUFA and 14.13% PUFA. [a]Values of each macronutrient are expressed in percentage of total energy content.
[b]AIN-93M vitamin mixture (g/100 g): thiamin HCl 0.06, ribofavin 0.06, pyridoxine HCl 0.07, niacin 0.3, calcium pantothenate 0.16, folic acid 0.02, biotin 2×10^{-3}, menadione sodium bisulfite 8×10^{-3}, sucrose 98.2, vitamin B_{12} 0.1, vitamin A (500,000 U/gm) 0.8, vitamin D_3 (400,000 U/gm) 25×10^{-3}, vitamin E acetate (50 U/gm) 1. gm: gram of matter
[c]AIN-93M mineral mixture (g/100 g): calcium phosphate 50, sodium chloride 7.4, potassium citrate 222, potassium sulfate 5.2, magnesium oxide 2.4, manganese carbonate 0.35, ferric citrate 0.6, zinc carbonate 0.16, cupric carbonate 0.03, potassium iodate 1×10^{-3}, sodium selenite 1×10^{-3}, chromium potassium sulfate 55×10^{-3}, sucrose 11.8.

After 15 days of diet adaptation, each group was divided into two other groups (n=6): Control, HFD, STZ and HFD-STZ. STZ and HFD-STZ groups received an intraperitoneal injection of streptozotocin (STZ) (40 mg/kg bw) (Sigma-Aldrich, St. Louis, MO, USA) dissolved in citrate buffer (0.1M, pH= 4.5), for 4 consecutive days. STZ was prepared immediately prior the injection. The two other groups: Control and HFD were injected only by vehicle solution (0.1 M citrate buffer, pH 4.5). After the final injection, glycemia was measured to confirm the establishment of hyperglycemia, typically characterized by fasting blood glucose levels exceeding 7.0 mmol/L (1.26 g/L).During the experimental period, mice had free access to water and diet.

Body weight, food and water intake were monitored weekly. At the end of the experiment which lasted 5 weeks, animals were fasted overnight then anesthetized with 2%isoflurane gas($C_3H_2ClF_5O$), sacrificed by cervical dislocation and fasting glycemia was determined from the tail vein by strips test (Accu-Chek Active, Roche Diagnostics, Mannheim, Germany). Tongues were cut from mice for papillae isolation. Blood plasma was collected and centrifuged at 1000g for 20 min at 4°C. Liver and adipose tissue were removed, rinsed with cold saline solution and weighed. All Samples were put in liquid nitrogen then stored at -80 °C until further analysis.

2.2. Two-bottle preference test

The experiments assessing spontaneous preference for a fatty acid solution were conducted using a two-bottle preference test, as previously described by Dramane et al. (2012).Six hours before the start of the experiment, mice were deprived of water intake. During the period of overnight, mice of each group were placed individually in cages, subjected to two bottles and they had to choose between a control and a test solution. The test solution included 0.2% linoleic acid (LA) (18:2 n-6) emulsified in 0.3 % xanthan gum (XG) (w/v) in water, while the control solution contained water with 0.3% XG (w/v).XG was used to emulsify the oil and to minimize differences of textural properties between both solutions. XG and LA were obtained from Sigma (St. Quentin Fallavier, France).

2.3. Papillae and taste bud cells isolation

Following the method previously described by El-Yassimi et al. (2008), taste bud cells (TBC) from lingual papillae were isolated using enzymatic digestion with a mixture of elastase and dispase (2 mg/mL each) in Tyrode's buffer (120 mM NaCl, 5 mMKCl, 10 mM HEPES, 1 mM $CaCl_2$, 10 mM glucose, 1 mM $MgCl_2$, 10

mM Na pyruvate, pH 7.4). The lingual papillae were carefully dissected under a microscope, and immediately after isolation, the TBC were used for calcium imaging experiments.

2.4. Biochemical analyses

2.4.1. Level of plasma insulin, HOMA-IR and QUICKI indices evaluation

An ultrasensitive ELISA (Enzyme-Linked Immunosorbent Assay) kit from Merck-Millipore (EMD Millipore; EZRMI-13K; Darmstadt, Germany) was used according for the determination of plasma insulin according to the manufacturer's instructions. It is based on the direct sandwich technique in which two monoclonal antibodies are directed against separate antigenic determinants on the insulin molecule. During incubation insulin in the sample reacts with enzyme (HRP)-conjugated anti-insulin antibody and anti-insulin antibody bound to microplate well. A simple washing step removes unbound enzyme labeled antibody. The bound HRP complex is detected by reaction with TMB substrate. The reaction is stopped by adding acid to give a colorimetric endpoint that is read using ELISA reader.
Homeostasis model assessment of insulin resistance index (HOMA-IR) was calculated according to the formula of Haffner et al. (1997):
HOMA-IR= fasting plasma glucose × fasting serum insulin/22.5.
Quantitative insulin sensitivity check index (QUICKI) was calculated according to the formula of Katz et al. (2000):
QUICKI = 1/ (log (fasting insulin) + log (fasting plasma glucose).

2.4.2. Plasma lipid profiles

Total Cholesterol (TC), triglycerides (TG) and high-density lipoprotein cholesterol (HDL-C) levels were determined by an enzymatic colorimetric assay, using commercial diagnostic kits (kit Biocon, Germany) and non-HDL cholesterol (non-HDL-C) is a calculated parameter derived by subtracting HDL-C from TC. Non-HDL cholesterol provides an estimation of all cholesterol containing (atherogenic) particles LDL, triglyceride-rich very low density lipoprotein and so-called remnant particles), thus providing a more accurate assessment of cardiovascular risk compared to LDL alone.

2.4.3. Plasma and tissue lipid peroxidation assessment

Plasma lipid peroxidation was assessed according to the method of Quintanilha et al. (1982) by the estimation of thiobarbituric acid reactive substances (TBARS). Malondialdehyde (Sigma-Aldrich, l'Isle d'Abeau, France) was used as a standard. One milliliter of diluted plasma was added to 2ml of thiobarbituric acid (TBA) (final concentration, 0.017 mmol/l), plus butylated hydroxytoluene (concentration, 3.36 µmol/l), the mixture was incubated at 100°C for 15 minutes. Following centrifugation (1,000 g for 10 min at 4°C), the absorbance of the supernatant was determined at 535 nm.

In tissues, TBARS was measured by the complex formed between malondialdehyde (MDA) and TBA (Ohkawa et al., 1979). Briefly, 0.5g of tissue (liver or adipose tissue) was homogenized with 4.5 mL of KCl (1.15%). 0.1 ml of sodium dodecylsulfate (8.1%), 750 µl of acetic acid (20%), and 750 µl of TBA reagent (0.8%) were added to 100µl of homogenate and mixed. The reaction mixture was incubated at 95°C for 60 min. Then it was cooled in ice and supplemented with 2.5 ml of n-butanolpyridine (15:1**).** The sample was mixed, centrifuged at 4000g for 10 minutes**.** The upper phase was collected and used for measuring the absorbance at 532nm.

2.4.4. Total antioxidant capacity

The total antioxidant capacity (T-AOC) was assayed by using colorimetric assay Kit (FRAP Method). Under acid condition Fe^{3+}-TPTZ can be reduced by antioxidants and produce blue Fe^{2+} and the antioxidant capacity of sample was determined by detection the absorbance at 593nm (MyBioSource, MyBioSource Inc., San Diego, CA, USA).

2.4.5. Superoxide dismutase activity

Superoxide dismutase (SOD, EC. 1.15.1.1) is a metalloenzyme that catalyses the dismutation of the supeoxideanion to molecular oxygen and hydrognperoxide.Atetrazolium salt was utilized in the assay for superoxide dismutase (kit Cayman,Cayman Chemicals, Ann Arbor, MI (USA)) to detect superoxide radicals

generated by hypoxanthine and xanthine oxidase. One unit of SOD was defined as the amount of enzyme needed to exhibit 50% dismutation of the superoxide radical. The absorbance value was recorded at 440 to 460nm.

2.4.6. Glutathion peroxidase activity

Glutathione peroxidase (GPx, EC 1.11.1.9) is a selenoenzyme that reduces hydroperoxides, including hydrogen peroxide, to water or alcohols using reduced glutathione (GSH) as a substrate. This activity is vital for protecting cells from oxidative stress. The GPx assay (kit Cayman, Cayman Chemicals, Ann Arbor, MI (USA)) employs a coupled reaction with glutathione reductase (GR), where GPx oxidizes GSH to glutathione disulfide (GSSG), which is then recycled to GSH by GR in the presence of NADPH. GPx activity is measured by monitoring the decline in absorbance at 340 nm, reflecting NADPH oxidation. One unit of GPx is defined as the enzyme amount oxidizing 1 µmol of NADPH per minute under standard conditions.

2.4.7. Measurement of proinflammatory cytokines:

An in vitro ELISA kits were used for the determination of quantitative measurement of mouse Interleukin-1 beta (IL-1β) (Cat. No: MBS824958), Interleukin-6 (IL-6)(Cat. No:MBS824703) or Tumor necrosis factor-alpha (TNF-α) (Cat. No: MBS825075) in plasma (MyBioSource, MyBioSource Inc., San Diego, CA, USA). These assays employ an antibody specific for Mouse IL-1β, IL-6 or TNF-α coated on a 96-well plate. Standards and samples are pipetted into the wells and IL-1β, IL-6 or TNF-α present in a sample are bound to the wells by the specific immobilized antibody. The wells are washed and biotinylated anti-Mouse IL-1β, IL-6 or TNF-α antibody are added. After washing away unbound biotinylated antibody, HRP-conjugated streptavidin is pipetted to the wells. The wells are again washed, a TMB substrate solution is added to the wells and color develops in proportion to the amounts of IL-1β, IL-6 or TNF-α bound. The Stop Solution changes the color from blue to yellow, and the intensity of the color is measured at 450 nm.

2.5. Measurement of Ca^{2+} signaling

As described previously by Dramane et al. (2012), isolated TBC were cultured in Willico-Dish wells containing RPMI complete medium, 10% fetal calf serum, 2 mM glutamine, 50 µg/mL penicillin–streptomycin, and 20 mM HEPES, at 37 °C. Following an overnight incubation, the supernatant was discarded. The cells were further incubated for 30 min with 1µM of Fura-2/AM in a buffer containing: 110 mM NaCl, 5.4 mM KCl, 25 mM $NaHCO_3$, 0.8 mM $MgCl_2$, 0.4 mM KH_2PO_4, 20 mMHepes, 1.2 mM $CaCl_2$, 10 mM Glucose pH 7.4 at 37°C. After the addition of test molecules to the wells, a Nikon TiU microscope employing a 40X oil immersion S-fluor objective (Nikon, Tokyo, Japan) was used to observe the fluctuations of intracellular free Ca^{2+} measured as the F_{340}/F_{380} ratio. Equipped with Luca-S EM-CCD camera, the microscope could record real-time digital images with 16-bit resolution. ΔRatio served as a measure of the fluctuations in intracellular free $Ca^{2+}$and it was calculated as the difference between the F_{340} and F_{380}.

2.6. Statistical analysis

All calculations were carried out with six independent measures for each set of samples by calculating means ± standard error of the mean (SEM) with the Statistica 8.1 software. The significance of differences between groups was evaluated by using o two way ANOVA and Tukey's honestly significant difference (HSD) test were performed to determine statistically significant differences between mean values ($p<0.05$): [a]HFD vs Control, [b]STZ vs Control, [c]HFD-STZ vs Control, [d]HFD vs STZ, [e]HFD-STZ vs STZ, [f]HFD-STZ vs HFD.

3. Results

In a study conducted on male C57BL/6J mice, the STZ group demonstrated significantly higher food intake ($p<0.05$) and energy intake ($p<0.001$) compared to the control group **(table 2)**. The HFD and HFD-STZ groups showed a significantly lower food intake than the control group ($p<0.001$). However, both the HFD and HFD-STZ groups had significantly higher energy intake ($p<0.001$) compared to the control group. Additionally, there was a significant increase in both food and energy intake in the HFD and HFD-STZ groups when compared to the STZ group ($p<0.001$). The HFD-STZ group had a higher energy intake than the HFD group ($p<0.01$). Conversely, there was no statistically significant difference in food consumption between these two groups.

Upon comparing the different groups, it was noted that the HFD group showed a 19% increased in body weight compared to the control group. The HFD-STZ group had a 13% lower body weight compared to the HFD group and a 14% reduction when compared to the STZ group. Remarkably, the HFD group exhibited a substantial 25% increase in body weight compared to the STZ group (table 2).
The relative liver weight comparisons were shown in table 2 revealed notable differences among the groups. The HFD group showed a 26% increase in relative liver weight compared to the control group, while the STZ group exhibited a 17% decrease. The HFD-STZ group had a 12% higher relative liver weight than the control group but demonstrated a 17% decrease compared to the HFD group. Additionally, the HFD-STZ group induced a 26% increase as compared to the STZ group. Most significantly, the HFD group showed a 40% rise in liver weight compared to the STZ group.

Table 2. Body weight, food consumption, energy intake, relative organ weights of liver and adipose tissue, fasting glycemia and insulinemia, HOMA-IR and QUICKI indices of mice at the end of the experiment

Groups	Control	HFD	STZ	HFD-STZ
Body weight (g)	26.82±0.42	33.06±0.55[a,d]	24.67±0.82[b]	28.60±0.33[c,e,f]
Food consumption (g/day/mouse)	5.11±0.12	3.76±0.10[a,d]	4.76±0.14[b]	3.91±0.15[c,e]
Energy intake (Kcal/day/mouse)	18.37±0.32	20.18±0.16[a,d]	17.11±0.23[b]	20.98±0.17[c,e,f]
Relative organ weights				
Liver	3.82±0.11	5.15±0.14[a,d]	3.16±0.25 [b]	4.26±0.11[c,e,f]
Adipose tissue	1.26±0.13	2.82±0.18[a,d]	1.09±0.16	2.52±0.13[c,e]
Glycemia (mmol/L)	5.12±0.14	9.21±0.50[a,d]	7.31±0.20[b]	10.32±0.35[c,e]
Insulinemia (□IU/mL)	4.34±0.35	13.91±0.34[a,d]	8.89±0.43[b]	11.16±0.25[c,e,f]
HOMA-IR	0.99±0.16	5.69±0.17[a,d]	2.89±0.13[b]	5.12±0.11[c,e,f]
QUICKI	0.38±0.02	0.30±0.01[a]	0.33±0.01[b]	0.30±0.03[c]

Values are means ± SEM of 6 mice per group. The Tukey test was used for statistical analysis, with a significance threshold set at $p < 0.05$.Statistical comparisons were made as follows: [a]HFD vs Control, [b]STZ vs Control, [c]HFD-STZ vs Control, [d]HFD vs STZ, [e]HFD-STZ vs STZ, [f]HFD-STZ vs HFD

Relative weight = [organ weight/body wheight] x 100.

Our findings also revealed a significant increase in the relative weight of adipose tissue in the HFD and HFD-STZ groups compared to the control group ($p<0.001$), with values 2.2- and 2-fold higher, respectively. Furthermore, both the HFD and HFD-STZ groups had significantly higher relative weights of adipose tissue compared to the STZ group ($p<0.001$), with values 2.6- and 2.3-fold higher, respectively. In diabetic mice on a HFD (HFD-STZ group), no significant difference was found compared to the HFD group (table 2).
At the end of the experiment, fasting blood glucose levels in the STZ group increased by 30% compared to the control group, and this elevation was accompanied by a 51% increase in insulin levels (table 2). Both the HFD and HFD-STZ groups exhibited significantly higher fasting blood glucose levels and insulin release response compared to the control group ($p<0.001$). Compared to the STZ group, the HFD group exhibited significantly elevated fasting blood glucose ($p<0.01$) and insulin levels ($p<0.001$).
The combination of STZ injection and HFD feeding (HFD-STZ group) in mice, resulted in a significant increase in both fasting blood glucose ($p<0.01$) and insulin levels ($p<0.05$) compared to STZ-induced mice on a standard diet. In HFD-STZ group, no significant difference was noted in fasting blood glucose compared to HFD group. Nevertheless, insulinemia was increased significantly ($p<0.01$).

Based on these measurements, we calculated HOMA-IR and QUICKI. Our findings revealed that the HFD, STZ and HFD-STZ groups exhibited elevated HOMA-IR values compared to the control group. Also, both the HFD and HFD-STZ groups showed higher HOMA-IR values than the STZ group. Whereas, no significant changes in the HOMA-IR index was observed in HFD-STZ vs HFD group. Regarding the QUICKI index, values were increased in all experimental groups as compared to the control group.
As shown in table 3, plasma levels of TC, HDL-C, non-HDL-C, and TG increased by 46%, 32%, 54%, and 60%, respectively, in the HFD group compared to the control group. Similarly, in the HFD-STZ group, these plasma lipid concentrations were elevated by 46%, 36%, 53%, and 66%, respectively. Inversely, the STZ group showed a reduction of 59% in HDL-C and 10% in TC, but an increase in non-HDL-C (+13%) and TG (+56%) compared to the control group.

Table 3. Levels of plasma lipids and lipid peroxidation in plasma, liver and adipose tissue

Groups	Control	HFD	STZ	HFD-STZ
Plasma lipids				
Total cholesterol (mmol/L)	1.85±0.12	3.40±0.28[a,d]	1.68±0.23	3.45±0.23[c,e]
HDL-cholesterol (mmol/L)	0.86±0.02	1.26±0.11[a,d]	0.54±0.04[b]	1.35±0.09[c,e]
Non-HDL cholesterol (mmol/L)	0.99±0.03	2.14±0.05[a,d]	1.14±0.02[b]	2.10±0.08[c,e]
Triglycerides (mmol/L)	1.24±0.10	3.12±0.13[a]	2.85±0.15b[b]	3.65±0.14[c,e,f]
Lipid peroxidation				
Plasma (nmol/mL)	48.41±1.28	67.91±0.71[a]	65.40±3.67[b]	77.10±2.40[c,e,f]
Liver (nmol/mg proteins)	46.40±0.57	66.30±1.12[a]	66.70±0.71[b]	67.10±1.84[c]
Adipose tissue (nmol/mg proteins)	43.01±1.41	54.80±1.70[a,d]	41.10±1.56	65.20±0.85[c,e,f]

Values are means ± SEM of 6 mice per group. The Tukey test was used for statistical analysis, with a significance threshold set at $p < 0.05$. Statistical comparisons were made as follows: [a]HFD vs Control, [b]STZ vs Control, [c]HFD-STZ vs Control, [d]HFD vs STZ, [e]HFD-STZ vs STZ, [f]HFD-STZ vs HFD

The HFD group exhibited elevated plasma TC (50%), HDL-C (66%), and non-HDL-C (47%) levels, with no significant difference in TG content compared to the STZ group. In addition, the HFD-STZ group demonstrated significant increases in plasma TC (+51%), HDL-C (+60%), non-HDL-C (+46%), and TG (+22%) compared to the STZ group. Whereas, no significant differences in plasma TC, HDL-C, and non-HDL-C levels were observed between diabetic mice on HFD (HFD-STZ group) and those on HFD alone (HFD group). Nevertheless, plasma TG concentrations were significantly increased by 14% in the HFD-STZ group compared to the HFD group.
Our data showed that in the STZ group compared to the control group, TBARS levels increased by 26% in plasma and 30% in the liver, with no significant difference in adipose tissue. Also, the HFD group exhibited elevated TBARS concentrations by 29%, 30%, and 21% in plasma, liver, and adipose tissue, respectively, compared to the control group. In the HFD-STZ group, TBARS levels remained elevated in plasma (+37%), liver (+31%), and adipose tissue (+34%) compared to the control group **(table 3)**.
The HFD group showed a 25% increase in adipose tissue TBARS concentrations compared to the STZ group, with no significant differences in plasma and liver. Compared to diabetic mice (STZ group), TBARS levels were significantly increased in plasma ($p<0.01$) and adipose tissue ($p<0.001$) in the HFD-STZ group, with no significant difference in the liver. In the HFD-STZ group, TBARS levels were elevated in both plasma (+12%) and adipose tissue (+16%) compared to the HFD group, with no significant difference in the liver **(table 3)**.
The study revealed a significant reduction in plasma T-AOC in the HFD, STZ, and HFD-STZ groups when compared to the control group, indicating a compromised antioxidant defense in these groups **(table 4)**. Notably, the HFD-STZ group showed higher T-AOC than the HFD group, suggesting that the combination of

a HFD and STZ-induced diabetes may partially counteract the reduction in antioxidant capacity observed in the HFD group alone.

Table 4. Assessment of plasma total antioxidant capacity (T-AOC), antioxidant enzyme activities, and proinflammatory cytokine levels

Groups	Control	HFD	STZ	HFD-STZ
Plasma T-AOC (mmol/L)	1.61±0.13	0.60±0.15[a]	1.22±0.11[b]	0.85±0.10[c,f]
Antioxidant enzymes activities				
Liver				
SOD (U/mg de proteins)	30.55±1.12	10.42±0.51[a,d]	17.12±0.62[b]	14.22±0.23[c,e,f]
GPx(U/mg de proteins)	23.33±2.19	8.23±0.25[a,d]	12.23±1.58[b]	10.61±0.15[c]
Adipose tissue				
SOD (U/mg de proteins)	23.55±2.11	11.47±1.52[a,d]	16.11±1.44[b]	12.55±1.26[c]
GPx (U/mg de proteins)	10.17±1.33	5.11±0.88[a,d]	8.33±1.09	6.77±0.45[c]
Pro-inflammatory cytokines				
IL-1□ (pg/mL plasma)	7.71±2.31	50.30±14.11[a]	33.51±1.79	79.37±21.50[c,e]
IL-6 (pg/mL plasma)	9.27±3.37	35.88±11.36[a]	30.55±2.48[b]	52.79±9.83[c,e]
TNF-α (pg/mL plasma)	7.47±3.22	30.44±3.55[a]	22.44±3.30[b]	42.44±2.02[c,e,f]

Values are means ± SEM of 6 mice per group. The Tukey test was used for statistical analysis, with a significance threshold set at $p < 0.05$.Statistical comparisons were made as follows: [a]HFD vs Control, [b]STZ vs Control, [c]HFD-STZ vs Control, [d]HFD vs STZ, [e]HFD-STZ vs STZ, [f]HFD-STZ vs HFD.
IL-1□: Interleukin-1□, IL-6: Interleukin-6, TNF-α: Tumor Necrosis Factor.

Regarding pro-inflammatory cytokines (table 4), the STZ group exhibited significantly elevated plasma levels of TNF-α ($p<0.01$) and IL-6 ($p<0.05$) compared to control, indicating a heightened inflammatory response. IL-1□ levels, however, did not show a significant change. In the HFD vs control group, there was a notable increase in IL-1□, IL-6, and TNF-α levels ($p<0.001$), reflecting the pro-inflammatory effects of a HFD. The HFD-STZ group displayed even higher levels of IL-1□, IL-6, and TNF-α compared to the control group ($p<0.001$), with a significant increase in TNF-α levels compared to the HFD group ($p<0.01$), highlighting the exacerbated inflammatory state in this group.
The evaluation of antioxidant enzymes (table 4) showed a substantial reduction in SOD activity in both the liver and adipose tissue in the STZ, HFD, and HFD-STZ groups as compared to control. Specifically, SOD activity in the liver was decreased by 44% in the STZ group and by 66% in the HFD group, with the HFD-STZ group showing a 53% reduction. In adipose tissue, SOD activity was decreased by1.5- fold in the STZ group and by 2.1-fold in the HFD group, while the HFD-STZ group exhibited a 1.9-fold reduction. Interestingly, the HFD-STZ group exhibited significantly higher liver SOD activity ($p<0.001$) compared to the HFD group, though no significant difference was noted in adipose tissue between these groups.
Regarding GPx activity, the STZ group exhibited a significant reduction in the liver ($p<0.001$) but not in adipose tissue compared to control. The HFD group showed a pronounced decrease in GPx activity in both the liver ($p<0.001$) and adipose tissue ($p<0.01$). The HFD-STZ group demonstrated an even more substantial reduction in liver GPx activity ($p<0.001$) and a moderate decrease in adipose tissue ($p<0.05$) as compared to the control group. However, when comparing the HFD-STZ group to the STZ and HFD groups, no significant differences in GPx activity were observed in either liver or adipose tissue (table 4).
A two-bottle preference test was employed to evaluate fat preference in mice (figure 1). The results demonstrated that mice on a standard diet (control group) displayed a pronounced preference for LA solution ($p<0.01$). Moreover, the STZ-induced diabetic mice showed a slight preference for the fat solution (LA)

compared to Xanthan gum (XG) ($p<0.05$). However, in this group LA preference was markedly diminished compared to the control group ($p<0.05$). Interestingly, in HFD or HFD-STZ mice, no significant difference was noted between both solutions, these groups lost preference for fat.

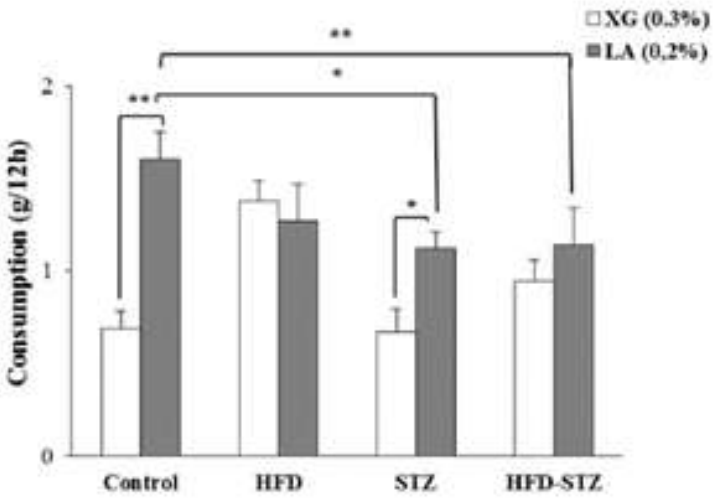

Figure 1. The two-bottle preference test assessment.

Two-bottle preference test was employed to evaluate fat preference in mice. Animals were subjected to two bottles for 12h/overnight. The test solution included 0.2% Linoleic acid (**LA**) emulsified in 0.3% Xanthan gum (**XG**). The control solution contained water with 0.3% XG (w/v). Values are means ± SEM of 6 mice per group. The Tukey test was used for statistical analysis, with a significance threshold set at $p<0.05$.

As shown in **figure 2**, LA triggered a rapid elevation in intracellular calcium levels in TBC from the control group. This response was decreased but not completely abolished in TBC from STZ group. However, in the HFD or HFD-STZ groups LA-induced increases of intracellular calcium concentration was completely abolished. \

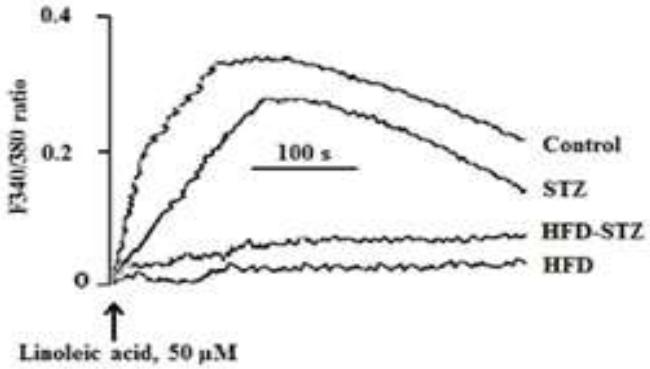

Figure 2. Intracellular calcium measurement.

Effect of linoleic acid (**LA**) on the changes in intracellular calcium in TBC from Control, STZ, HFD and HFD-STZ groups. As described in materials and methods, the changes in intracellular calcium (**F340/F380**) are shown in response to LA stimulation at 50µM in isolated TBC from mice papillae of each group (n=6).

4. Discussion

In this study, we investigated the impact of a high-fat diet (HFD) combined with hyperinsulinemia on fat taste perception in taste bud cells (TBC), with particular emphasis on calcium signaling dysfunctions. Additionally, we examined the synergistic effects of combination of HFD and diabetes induced by STZ on critical metabolic parameters, including insulin resistance, hyperglycemia, dyslipidemia, oxidative stress (OS), and inflammation, a key characteristic of type 2 diabetes (T2D) progression. Our study identified significant differences in body weight (BW) across the groups, highlighting the complex metabolic interactions between HFD and STZ treatment.

Rodent models maintained on high-fat diets are commonly used in cardiovascular disease research. Specifically, Wistar/Sprague-Dawley rats and C57BL/6 mice fed HFD are widely employed to study diet-induced obesity (DIO) and insulin resistance due to their increased susceptibility to metabolic disturbances (Fontaine et al., 2016). The HFD group showed an increase in BW compared to the control group, consistent with the obesogenic properties of high-fat diets. Li et al. (2012) reported that combining HFD with STZ-induced diabetes led to elevated blood glucose, lipids, and BW in mice. Similarly, Ji et al. (2023) attributed weight gain to higher caloric intake and impaired energy balance, which enhanced fat storage. Rodents fed an HFD for five weeks gained body weight and adjusted their body composition to accommodate excess energy intake, underscoring the variability in nutrient utilization that contributes to metabolic inefficiency and weight gain (Milhem, 2024). Conversely, the STZ group showed reduced body weight, consistent with findings by Guo et al. (2018) in a rat model.

In our study, the HFD-STZ group exhibited an intermediate BW phenotype, suggesting a complex interaction between HFD and STZ. While the HFD promotes weight gain by increasing fat storage, the hyperglycemic and catabolic state induced by STZ counteracts this effect, leading to a reduced weight gain. Similar observations were made by Zhang et al. (2008), who found no significant BW difference between HFD-fed rats treated with low doses of STZ and controls. Conversely, Byrne et al. (2015) observed that HFD-fed rats treated with STZ experienced weight loss due to the catabolic effects of hyperglycemia. Our study also revealed significant metabolic changes in the HFD-STZ model, corroborating the findings of Vatandoust et al. (2018), who induced T2D in rats with a combination of high-fat, high-carbohydrate diets and STZ treatment.

Regarding liver weight, the HFD group showed an increase, suggesting hepatic steatosis, a well-established consequence of high-fat diets. Meijer et al. (2010) emphasized the role of dietary fat content in the development of hepatic steatosis, regardless of caloric intake. Echeverría et al. (2019) found that HFD-fed mice exhibited liver oxidative stress and mitochondrial dysfunction, contributing to steatosis. In contrast, the STZ group showed reduced liver weight, likely due to the catabolic effects of insulin deficiency. Although direct studies linking STZ-induced insulin deficiency to decreased liver weight are limited, it is well-documented that insulin deficiency increases protein catabolism, leading to weight loss, which may affect liver tissue as well. Both the HFD and HFD-STZ groups exhibited higher adipose tissue weight than the control, consistent with the role of high-fat diets in promoting visceral fat accumulation and metabolic dysfunction (Hariri and Thibault, 2010).

When assessing food consumption and energy intake, the STZ group exhibited significantly higher food intake than the HFD and HFD-STZ groups, a hallmark of hyperphagia due to insulin deficiency (Sen et al., 2011). Despite this, the STZ group had reduced energy intake, suggesting that while total food volume decreased, the caloric density of the diet contributed to metabolic imbalance and weight gain. This is supported by Magalhães et al. (2019), who found that rats subjected to HFD and STZ injections showed increased energy intake despite reduced food volume, leading to metabolic disturbances.

In terms of fat taste perception, both the HFD and HFD-STZ groups lost preference for fat solution. Additionally, linoleic acid (LA) stimulation in TBC failed to induce a significant increase in intracellular calcium concentration ($[Ca^{2+}]_i$). This aligns with Djeziri et al. (2018), who reported that chronic HFD exposure in mice reduces fat preference, likely due to altered $[Ca^{2+}]_i$. Lipid sensors, such as CD36 and GPR120, play a critical role in fat taste perception, and their dysregulation may impair fat preference (Muthuswamy et al., 2024). Ozdener et al. (2014) found that obese mice exhibited reduced fat preference, correlating with decreased $[Ca^{2+}]_i$ and CD36 receptor expression in TBC. Additionally, Maliphol et al. (2013)

demonstrated that diet-induced obesity (DIO) in mice reduces taste receptor responsiveness, particularly to sweet tastes, which could contribute to altered dietary preferences and exacerbate hyperglycemia.

Our study also investigated the relationship between fat taste perception and blood insulin levels. The HFD, STZ, and HFD-STZ groups showed higher insulin levels compared to the control group. This hyperinsulinemia was associated to a reduced preference for fat and a decrease of $[Ca^{2+}]_i$ induced by LA in TBC in the STZ group when compared to the control group. This suggests a relationship between fat taste sensitivity and elevated blood insulin levels. Moreover, studies have highlighted the impact of insulin on taste sensitivity, with higher insulin levels potentially inhibiting taste progenitor cell growth and affecting some taste sensitivities (Doyle et al., 2018; Takai et al., 2019).

Regarding glucose metabolism, STZ treatment induced a significant increase in fasting blood glucose and insulin levels compared to the control. Both the HFD and HFD-STZ groups showed elevated glycemia and insulinemia, consistent with the role of HFD in promoting insulin resistance and impaired glucose metabolism. Racine et al. (2024) reported that a combination of HFD and low-dose STZ induces hyperinsulinemia and insulin resistance in male C57BL/6J mice. Our findings align with Gheibi et al. (2017), who observed that low-dose STZ injections result in partial destruction of pancreatic β cells, leading to hyperglycemia in animals fed an HFD. To assess insulin resistance, we used the Homeostatic Model Assessment for Insulin Resistance (HOMA-IR). Our results revealed significantly higher HOMA-IR values in the HFD, STZ and HFD-STZ groups compared to the control. Notably, the HFD and HFD-STZ groups exhibited higher HOMA-IR values than the STZ group. Andonova et al. (2023) reported an increase in HOMA-IR and a concomitant decrease in HOMA-β, suggesting the development of insulin resistance and impaired beta-cells function in rats subjected to a HFD and a single dose of STZ.

Our findings also showed impaired lipid profiles in the HFD and STZ groups with decreased HDL-C and total cholesterol (TC) levels in STZ vs control group, while, non-HDL-C and triglycerides (TG) were elevated, these results are consistent with the dyslipidemia observed in T2D **(**Magalhães et al., 2019). Both the HFD and HFD-STZ groups exhibited elevated TC, non-HDL-C, TG, and reduced HDL-C levels compared to the control, corroborating previous research showing that HFD feeding exacerbates dyslipidemia in STZ-induced diabetic mice (Wang et al., 2021).

The study also highlighted oxidative stress, with a significant reduction in plasma total antioxidant capacity (T-AOC) in the HFD, STZ, and HFD-STZ groups. Interestingly, the HFD-STZ group showed a higher T-AOC than the HFD group alone, suggesting that the combination of HFD and STZ-induced diabetes partially mitigates the reduction in antioxidant capacity observed with HFD alone. Moreover, lipid peroxidation products, measured by thiobarbituric acid reactive substances (TBARS), were elevated in the HFD and HFD-STZ groups compared to the control.

Oxidative stress (OS) plays a central role in the pathogenesis of T2D and metabolic syndrome (He et al., 2023). Our study found reduced activity of antioxidant enzymes superoxide dismutase (SOD) and glutathione peroxidase (GPx) in all experimental groups compared to the control, particularly in the liver and adipose tissue of the HFD-STZ group. This highlights the exacerbation of oxidative damage in the combined HFD and STZ model, consistent with previous research linking HFD-induced oxidative stress to impaired antioxidant defense (Lee et al., 2009; Lasker et al., 2019).

This heightened inflammatory response likely amplified oxidative stress and metabolic disturbances, further impairing taste perception. Systemic inflammation has been shown to influence the regeneration and functionality of taste cells by affecting progenitor cell proliferation and differentiation (Takai et al., 2019). Pro-inflammatory cytokines are known to disrupt calcium homeostasis and impair receptor sensitivity in various tissues, including the gustatory system. Additionally, Obesity-induced low-grade inflammation alters the normal balance of proliferation and cell death in taste bud cells, resulting in a reduction in taste bud abundance and an inhibition of regeneration in C57BL/6 mice **(**kaufman et al., 2018). Moreover, the combination of HFD and STZ-induced diabetes aggravates insulin resistance, dyslipidemia, and oxidative stress, which may lead to cumulative damage to gustatory tissues. These disruptions may contribute to the reduced expression of lipid-sensing receptors, such as CD36 and GPR120, observed in obese models, ultimately leading to diminished taste sensitivity for dietary fats (Ozdener et al., 2014). Our study demonstrated that HFD feeding and STZ-induced hyperglycemia triggered inflammatory responses, as

evidenced by elevated levels of IL-1, IL-6, and TNF-α in the HFD and STZ groups. Notably, the HFD-STZ group showed even higher cytokine levels, suggesting that the combination of these factors exacerbates systemic inflammation, which is strongly linked to T2D and its complications (Jin et al., 2024).

In conclusion, our research offers valuable insights into the interplay between taste perception and metabolic health. The combination of HFD and STZ-induced diabetes drives a cascade of metabolic dysfunctions, including insulin resistance, lipid dysregulation, heightened oxidative stress, and systemic inflammation. Future studies should further explore the role of insulin signaling in oral tissues particularly its influence on fat taste sensitivity, alongside exploring therapeutic avenues such as antioxidant and anti-inflammatory strategies, as well as customized dietary interventions, to mitigate the detrimental effects of HFD and STZ-induced diabetes. Long-term research is crucial to uncovering the pathways through which these stressors accelerate disease progression, with the potential for identifying innovative therapeutic targets for T2D and its related complications.

Acknowledgments

The authors express their gratitude to the Algerian Ministry of Higher Education and Scientific Research (MESRS) and the Directorate General for Scientific Research and Technological Development (DGRSDT-MESRS) for their support.

Conflict of Interest

All authors declare that there is no conflict of interest.

References

1. American Diabetes Association Professional Practice Committee (2024). Standards of Care in Diabetes-2024. Diabetes Care 47 (Suppl 1), S20–S42. https://doi.org/10.2337/dc24-S002
2. Andonova, M., Dzhelebov, P., Trifonova, K., Yonkova, P., Kostadinov, N., Nancheva, K., Ivanov, V., Gospodinova, K., Nizamov, N., 3. Tsachev, I. et Chernev, C. (2023). Metabolic Markers Associated with Progression of Type 2 Diabetes Induced by High-Fat Diet and Single Low Dose Streptozotocin in Rats. Vet Sci, 10(7), 431. https://doi.org/10.3390/vetsci10070431
3. Baquero, A. F. et Gilbertson, T. A. (2011). Insulin activates epithelial sodium channel (ENaC) via phosphoinositide 3-kinase in mammalian taste receptor cells. Am J Physiol Cell Physiol, 300(4), C860–C871. https://doi.org/10.1152/ajpcell.00318.2010
4. Bartolomé, A. (2023). The Pancreatic Beta Cell: Editorial. Biomolecules, 13(3), 495. https://doi.org/10.3390/biom13030495
5. Byrne, F. M., Cheetham, S., Vickers, S. et Chapman, V. (2015). Characterisation of pain responses in the high fat diet/streptozotocin model of diabetes and the analgesic effects of antidiabetic treatments. J Diabetes Res, 2015, 752481. https://doi.org/10.1155/2015/752481
6. de Meijer, V. E., Le, H. D., Meisel, J. A., Akhavan Sharif, M. R., Pan, A., Nosé, V. et Puder, M. (2010). Dietary fat intake promotes the development of hepatic steatosis independently from excess caloric consumption in a murine model. Metabolism, 59(8), 1092–1105.
7. https://doi.org/10.1016/j.metabol.2009.11.006
8. Djeziri, F. Z., Belarbi, M., Murtaza, B., Hichami, A., Benammar, C. et Khan, N. A. (2018). Oleanolic acid improves diet-induced obesity by modulating fat preference and inflammation in mice. Biochimie, 152, 110–120. https://doi.org/10.1016/j.biochi.2018.06.025
9. Doyle, M. E., Fiori, J. L., Gonzalez Mariscal, I., Liu, Q. R., Goodstein, E., Yang, H., Shin, Y. K., Santa-Cruz Calvo, S., Indig, F. E. et Egan, J. M. (2018). Insulin Is Transcribed and Translated in Mammalian Taste Bud Cells. Endocrinology, 159(9), 3331–3339. https://doi.org/10.1210/en.2018-00534
10. Dramane, G., Abdoul-Azize, S., Hichami, A., Vögtle, T., Akpona, S., Chouabe, C., Sadou, H., Nieswandt, B., Besnard, P. et Khan, N. A. (2012). STIM1 regulates calcium signaling in taste bud cells and preference for fat in mice. J Clin Invest, 122(6), 2267–2282. https://doi.org/10.1172/JCI59953
11. Drewnowski, A. (1997). Taste preferences and food intake. Annu Rev Nutr, 17(1), 237-253.
12. Echeverría, F., Valenzuela, R., Bustamante, A., Álvarez, D., Ortiz, M., Espinosa, A., Illesca, P., Gonzalez-Mañan, D. et Videla, L. A. (2019). High-fat diet induces mouse liver steatosis with a concomitant decline in energy metabolism: attenuation by eicosapentaenoic acid (EPA) or hydroxytyrosol (HT) supplementation and the additive effects upon EPA and HT co-administration. Food Funct, 10(9), 6170–6183.
13. https://doi.org/10.1039/c9fo01373c

14. El-Yassimi, A., Hichami, A., Besnard, P. et Khan, N. A. (2008). Linoleic acid induces calcium signaling, Src kinase phosphorylation, and neurotransmitter release in mouse CD36-positive gustatory cells. J Biol Chem, 283(19), 12949-12959. https://doi.org/10.1074/jbc.M707478200
15. Fernández-Millán, E. et Guillén, C. (2022). Multi-Organ Crosstalk with Endocrine Pancreas: A Focus on How Gut Microbiota Shapes Pancreatic Beta-Cells. Biomolecules, 12(1), 104.
16. https://doi.org/10.3390/biom12010104
17. Fontaine, D. A. et Davis, D. B. (2016). Attention to Background Strain Is Essential for Metabolic Research: C57BL/6 and the International Knockout Mouse Consortium. Diabetes, 65(1), 25–33. https://doi.org/10.2337/db15-0982
18. Galicia-Garcia, U., Benito-Vicente, A., Jebari, S., Larrea-Sebal, A., Siddiqi, H., Uribe, K. B., Ostolaza, H. et Martín, C. (2020). Pathophysiology of Type 2 Diabetes Mellitus. Int J Mol Sci, 21(17), 6275. https://doi.org/10.3390/ijms21176275
19. Gheibi, S., Kashfi, K. et Ghasemi, A. (2017). A practical guide for induction of type-2 diabetes in rat: Incorporating a high-fat diet and streptozotocin. Biomed Pharmacother, 95, 605–613. https://doi.org/10.1016/j.biopha.2017.08.098
20. Guo, X. X., Wang, Y., Wang, K., Ji, B. P. et Zhou, F. (2018). Stability of a type 2 diabetes rat model induced by high-fat diet feeding with low-dose streptozotocin injection. J Zhejiang Univ Sci B, 19(7), 559–569. https://doi.org/10.1631/jzus.B1700254
21. Haffner, S. M., Miettinen, H. et Stern, M. P. (1997). The homeostasis model in the San Antonio heart study. Diabetes Care, 20(7), 1087-1092. https://doi.org/10.2337/diacare.20.7.1087
22. Hariri, N. et Thibault, L. (2010). High-fat diet-induced obesity in animal models. Nutr Res Rev, 23(2), 270–299. https://doi.org/10.1017/S0954422410000168
23. He, L. Y., Li, Y., Niu, S. Q., Bai, J., Liu, S. J. et Guo, J. L. (2023). Polysaccharides from natural resource: ameliorate type 2 diabetes mellitus via regulation of oxidative stress network. Front Pharmacol, 14, 1184572. https://doi.org/10.3389/fphar.2023.1184572
24. Hichami, A., Khan, A. S. et Khan, N. A. (2022). Cellular and Molecular Mechanisms of Fat Taste Perception. Pharmacol, 275, 247–270. https://doi.org/10.1007/164_2021_437
25. Ji, T., Fang, B., Wu, F., Liu, Y., Cheng, L., Li, Y., Wang, R. et Zhu, L. (2023). Diet Change Improves Obesity and Lipid Deposition in High-Fat Diet-Induced Mice. Nutrients, 15(23), 4978. https://doi.org/10.3390/nu15234978
26. Jin, Z., Zhang, Q., Liu, K., Wang, S., Yan, Y., Zhang, B. et Zhao, L. (2024). The association between interleukin family and diabetes mellitus and its complications: An overview of systematic reviews and meta-analyses. Diabetes Res Clin Pract, 210, 111615. https://doi.org/10.1016/j.diabres.2024.111615
27. Katz, A., Nambi, S. S., Mather, K., Baron, A. D., Follmann, D. A., Sullivan, G. et Quon, M. J. (2000). Quantitative insulin sensitivity check index: a simple, accurate method for assessing insulin sensitivity in humans. J Clin Endocrinol Metab, 85(7), 2402–2410. https://doi.org/10.1210/jcem.85.7.6661
28. Kaufman, A., Choo, E., Koh, A. et Dando, R. (2018). Inflammation arising from obesity reduces taste bud abundance and inhibits renewal. PLoS Biol, 16(3), e2001959. https://doi.org/10.1371/journal.pbio.2001959
29. Khan, A. S., Keast, R. et Khan, N. A. (2020). Preference for dietary fat: From detection to disease. Prog Lipid Res, 78, 101032. https://doi.org/10.1016/j.plipres.2020.1010323
30. Lasker, S., Rahman, M. M., Parvez, F., Zamila, M., Miah, P., Nahar, K., Kabir, F., Sharmin, S. B., Subhan, N., Ahsan, G. U. et Alam, M. A. (2019). High-fat diet-induced metabolic syndrome and oxidative stress in obese rats are ameliorated by yogurt supplementation. Sci Rep, 9(1), 20026. https://doi.org/10.1038/s41598-019-56538-0
31. Lee, J. H., Son, C. W., Kim, M. Y., Kim, M. H., Kim, H. R., Kwak, E. S., Kim, S. et Kim, M. R. (2009). Red beet (Beta vulgaris L.) leaf supplementation improves antioxidant status in C57BL/6J mice fed high fat high cholesterol diet. Nutr. Res Pract, 3(2), 114–121. https://doi.org/10.4162/nrp.2009.3.2.114
32. Li, W., Zhang, M., Gu, J., Meng, Z. J., Zhao, L. C., Zheng, Y. N., Chen, L. et Yang, G. L. (2012). Hypoglycemic effect of protopanaxadiol-type ginsenosides and compound K on Type 2 diabetes mice induced by high-fat diet combining with streptozotocin via suppression of hepatic gluconeogenesis. Fitoterapia, 83(1), 192–198. https://doi.org/10.1016/j.fitote.2011.10.011
33. Magalhães, D. A., Kume, W. T., Correia, F. S., Queiroz, T. S., Allebrandt Neto, E. W., Santos, M. P. D., Kawashita, N. H. et França, S. A. (2019). High-fat diet and streptozotocin in the induction of type 2 diabetes mellitus: a new proposal. An Acad Bras Cienc, 91(1), e20180314. https://doi.org/10.1590/0001-3765201920180314
34. Maliphol, A. B., Garth, D. J. et Medler, K. F. (2013). Diet-induced obesity reduces the responsiveness of the peripheral taste receptor cells. PLoS One, 8(11), e79403. https://doi.org/10.1371/journal.pone.0079403
35. Melo, B. P., Zacarias, A. C., Oliveira, J. C. C., de Souza, L. M. C., Sabino, J., Ferreira, A. V. M., Tonoli, C., Dos Santos, M. L., de Avelar, G. F., Meeusen, R., Heyman, E. et Soares, D. D. (2021). Thirty days of combined consumption of a high-fat diet and fructose-rich beverages promotes insulin resistance and modulates inflammatory response and histomorphometry parameters of liver, pancreas, and adipose tissue in Wistar rats. Nutrition, 91-92, 111403. https://doi.org/10.1016/j.nut.2021.111403

36. Milhem, F., Skates, E., Wilson, M. et Komarnytsky, S. (2024). Obesity-Resistant Mice on a High-Fat Diet Display a Distinct Phenotype Linked to Enhanced Lipid Metabolism. Nutrients, 16(1), 171. https://doi.org/10.3390/nu16010171
37. Muthuswamy, K., Vasanthakumar, K., Panneerselvan, P., Thangamani, L., Krishnan, V., Piramanayagam, S. et Subramaniam, S. (2024). FAHFA promotes intracellular calcium signaling via activating the fat taste receptor, CD36 and Src protein kinases in mice taste bud cells. Biochim Biophys Acta Gen Subj, 1868(12), 130722. https://doi.org/10.1016/j.bbagen.2024.130722
38. Ninomiya, Y., Sako, N. et Imai, Y. (1995). Enhanced gustatory neural responses to sugars in the diabetic db/db mouse. Am J Physiol, 269(4 Pt 2), R930–R937. https://doi.org/10.1152/ajpregu.1995.269.4.R930
39. Ohkawa, H., Ohishi, N. et Yagi, K. (1979). Assay for lipid peroxides in animal tissues by thiobarbituric acid reaction. Anal Biochem, 95(2), 351-358. https://doi.org/10.1016/0003-2697(79)90738-3
40. Ozdener, M. H., Subramaniam, S., Sundaresan, S., Sery, O., Hashimoto, T., Asakawa, Y., Besnard, P., Abumrad, N. A. et Khan, N. A. (2014). CD36- and GPR120-mediated Ca^{2+} signaling in human taste bud cells mediates differential responses to fatty acids and is altered in obese mice. Gastroenterology, 146(4), 995–1005. https://doi.org/10.1053/j.gastro.2014.01.006
41. Peinado, B. R. R., Frazão, D. R., Bittencourt, L. O., de Souza-Rodrigues, R. D., Vidigal, M. T. C., da Silva, D. T., Paranhos, L. R., Magno, M. B., Fagundes, N. C. F., Maia, L. C. et Lima, R. R. (2023). Is obesity associated with taste alterations? A systematic review. Front Endocrinol (Lausanne), 14, 1167119. https://doi.org/10.3389/fendo.2023.1167119
42. Quintanilha, A. T., Packer, L., Davies, J. M., Racanelli, T. L. et Davies, K. J. (1982). Membrane effects of vitamin E deficiency: bioenergetic and surface charge density studies of skeletal muscle and liver mitochondria. Ann N Y Acad Sci, 393, 32–47. https://doi.org/10.1111/j.1749-6632.1982.tb31230.x
43. Racine, K. C., Iglesias-Carres, L., Herring, J. A., Wieland, K. L., Ellsworth, P. N., Tessem, J. S., Ferruzzi, M. G., Kay, C. D. et Neilson, A. P. (2024). The high-fat diet and low-dose streptozotocin type-2 diabetes model induces hyperinsulinemia and insulin resistance in male but not female C57BL/6J mice. Nutr Res, 131, 135–146. https://doi.org/10.1016/j.nutres.2024.09.008
44. Rohde, K., Schamarek, I. et Blüher, M. (2020). Consequences of Obesity on the Sense of Taste: Taste Buds as Treatment Targets? Diabetes Metab J, 44(4), 509–528. https://doi.org/10.4093/dmj.2020.0058
45. Sadri, H., Goodarzi, M. T., Saberi, Z., & Seifi, M. **(**2017). Antioxidant effects of biochanina in streptozotocin induced diabetic rats. Brazilian Archives of Biology and Technology, 60. https://doi.org/10.1590/1678-4324-2017160741
46. Sen, S., Roy, M., & Chakraborti, A. S. (2011). Ameliorative effects of glycyrrhizin on streptozotocin-induced diabetes in rats. Journal of Pharmacy and Pharmacology, 63(2), 287–296.
47. https://doi.org/10.1111/j.20427158.2010.01217.x
48. Singh, R., Gholipourmalekabadi, M., & Shafikhani, S. H**.** (2024). Animal models for type 1 and type 2 diabetes: advantages and limitations. Frontiers in Endocrinology (Lausanne), 15, 1359685.
49. https://doi.org/10.3389/fendo.2024.1359685
50. Sun, H., Saeedi, P., Karuranga, S., Pinkepank, M., Ogurtsova, K., Duncan, B. B., Stein, C., Basit, A., Chan, J. C. N., Mbanya, J. C., Pavkov, M. E., Ramachandaran, A., Wild, S. H., James, S., Herman, W. H., Zhang, P., Bommer, C., Kuo, S., Boyko, E. J., & Magliano, D. J. (2022). IDF Diabetes Atlas: Global, regional and country-level diabetes prevalence estimates for 2021 and projections for 2045. Diabetes Research and Clinical Practice, 183, 109119.
51. https://doi.org/10.1016/j.diabres.2021.109119
52. Takai, S., & Shigemura, N**.** (2020). Insulin function in peripheral taste organ homeostasis. Current Oral Health Reports, 7, 168-173. https://doi.org/10.1007/s40496-020-00266-2
53. Takai, S., Watanabe, Y., Sanematsu, K., Yoshida, R., Margolskee, R. F., Jiang, P., Atsuta, I., Koyano, K., Ninomiya, Y., & Shigemura, N. **(**2019). Effects of insulin signaling on mouse taste cell proliferation. PLOS ONE, 14(11), e0225190. https://doi.org/10.1371/journal.pone.0225190
54. Varghese, J., James, J. V., Anand, R., Narayanasamy, M., Rebekah, G., Ramakrishna, B., Nellickal, A. J., & Jacob, M. (2020). Development of insulin resistance preceded major changes in iron homeostasis in mice fed a high-fat diet. Journal of Nutritional Biochemistry, 84, 108441. https://doi.org/10.1016/j.jnutbio.2020.108441
55. Vatandoust, N., Rami, F., Salehi, A. R., Khosravi, S., Dashti, G., Eslami, G., Momenzadeh, S., & Salehi, R. (2018). Novel High-Fat Diet Formulation and Streptozotocin Treatment for Induction of Prediabetes and Type 2 Diabetes in Rats. Advances in Biomedical Research, 7, 107. https://doi.org/10.4103/abr.abr_8_17
56. Wang, P., Liu, Y., Zhang, T., Yin, C., Kang, S. Y., Kim, S. J., Park, Y. K., & Jung, H. W**.** (2021). Effects of Root Extract of Morinda officinalis in Mice with High-Fat-Diet/Streptozotocin-Induced Diabetes and C2C12 Myoblast Differentiation. ACS Omega, 6(41), 26959–26968.
57. https://doi.org/10.1021/acsomega.1c03372

58. Wickramasinghe, A. S. D., Attanayake, A. P., & Kalansuriya, P. (2022). Biochemical characterization of high fat diet fed and low dose streptozotocin induced diabetic Wistar rat model. Journal of Pharmacology and Toxicology Methods, 113, 107144. https://doi.org/10.1016/j.vascn.2021.107144
59. Yu, J. H., Shin, M. S., Lee, J. R., Choi, J. H., Koh, E. H., Lee, W. J., Park, J. Y., & Kim, M. S. (2014). Decreased sucrose preference in patients with type 2 diabetes mellitus. Diabetes Research and Clinical Practice, 104(2), 214–219.
60. https://doi.org/10.1016/j.diabres.2014.02.007
61. Zhang, M., Lv, X. Y., Li, J., Xu, Z. G., & Chen, L. (2008). The characterization of high-fat diet and multiple low-dose streptozotocin induced type 2 diabetes rat model. Experimental Diabetes Research, 2008, 704045. https://doi.org/10.1155/2008/704045